

# Striated surface morphology and crystal orientation of m-plane GaN films grown on $\gamma$ -LiAlO<sub>2</sub>(100)

K. R. Wang,<sup>1,a)</sup> M. Ramsteiner,<sup>1</sup> C. Mauder,<sup>2</sup> Q. Wan,<sup>1</sup> T. Hentschel,<sup>1</sup> H. T. Grahn,<sup>1</sup> H. Kalisch,<sup>2</sup> M. Heuken,<sup>2,3</sup> R. H. Jansen,<sup>2</sup> and A. Trampert<sup>1</sup>

<sup>1</sup>Paul-Drude-Institut für Festkörperelektronik, Hausvogteiplatz 5–7, 10117 Berlin, Germany

<sup>2</sup>Institut für Theoretische Elektrotechnik, RWTH Aachen University, Kackertstr. 15–17, 52072 Aachen, Germany

<sup>3</sup>AIXTRON AG, Kaiserstr. 98, 52134 Herzogenrath, Germany

(Received 5 April 2010; accepted 12 May 2010; published online 10 June 2010)

Polarized in-plane and cross-sectional Raman spectra have been used to determine the crystal orientation of m-plane GaN grown on  $\gamma$ -LiAlO<sub>2</sub>(100) (LAO) using a three-step metalorganic vapor phase epitaxy process. The epitaxial relationship is found to be GaN(1 $\bar{1}$ 00)∥LAO(100) and GaN[11 $\bar{2}$ 0]∥LAO[001]. However, the stripes on the GaN surface are oriented parallel to [0001], i.e., perpendicular to the one found on striated m-plane GaN surfaces in previous studies. This unusual orientation is attributed to the changes in the Ga adatom kinetics due to the presence of a 2-nm-thick interlayer observed at the GaN/LAO interface in transmission electron microscopy. © 2010 American Institute of Physics. [doi:10.1063/1.3449133]

M-plane (1 $\bar{1}$ 00) hexagonal GaN grown on tetragonal  $\gamma$ -LiAlO<sub>2</sub>(100) (LAO) has attracted much attention since related heterostructures are free of spontaneous and piezoelectric polarizations.<sup>1</sup> The absence of the quantum-confined Stark effect and its consequences are prerequisites for the production of brighter light emitters.<sup>2,3</sup>

The surface morphology of heteroepitaxially deposited m-plane GaN exhibits elongated stripe features.<sup>4–8</sup> Both molecular-beam epitaxy (MBE) and hydride vapor phase epitaxy (HVPE) grown m-plane GaN films on LAO substrates show similar striated surfaces with slates orientated parallel to [11 $\bar{2}$ 0].<sup>4–8</sup> The possible origins of this anisotropic surface are (i) the replication of the substrate morphology,<sup>5</sup> (ii) the Ga adatom kinetics,<sup>7,9</sup> and (iii) extended defects, which are present mainly in the form of basal-plane stacking faults (BPSFs).<sup>6,8,10</sup> Recent theoretical work using the density-functional theory (DFT) indicates that the anisotropic slate-like surface morphology is influenced by the Ga adatom kinetics.<sup>9</sup> The calculated diffusion barrier oriented along [11 $\bar{2}$ 0] equals 0.21 eV, which is much smaller than the value of 0.93 eV along [0001].<sup>9</sup> As a consequence, the stripes oriented parallel to [11 $\bar{2}$ 0] can be explained in a reasonable manner.<sup>9</sup> In contrast, the existence of another growth mechanism has been reported for Ta on Ta(001), which leads to the formation of stripes along the direction of the larger diffusion barrier.<sup>11</sup>

In the present study, we investigate the surface morphology of m-plane GaN samples grown on LAO using metalorganic vapor phase epitaxy (MOVPE) and find that the GaN surfaces exhibit the typical striated morphology but with a stripe orientation that is different compared to the one commonly observed.<sup>4–8</sup>

Nonpolar m-plane GaN thin films are grown on LAO(100) by MOVPE using a three-step technique.<sup>12</sup> Prior

to growth, the LAO is exposed to flowing ammonia at 900 °C for 2 min (step 1). Subsequently, a 60 nm GaN is grown at 900 °C under a 300 mbar N<sub>2</sub> ambient (step 2). Finally, 1  $\mu$ m GaN is deposited under the same growth conditions using H<sub>2</sub> as the carrier gas (step 3). The molar V/III ratio is kept at 1,010 during the second and third steps of growth. Micro-Raman spectroscopy is employed to determine the crystal orientation of the m-plane GaN film. Using a spectrograph (800 mm focal length) with a single grating (600 lines/mm) monochromator, a spectral resolution of 4.5 cm<sup>-1</sup> is achieved. The spectra are excited by a He–Ne laser (632.8 nm) with the stray light suppressed by a notch filter. The surface morphology of the aligned sample is recorded using an optical microscope (OM) with contrast enhancement and atomic force microscopy (AFM) operated in tapping mode. Electron microscopy investigations are carried out using a JEOL 3010 transmission electron microscope (TEM) with conventional sandwiched specimens.

Figure 1(a) displays the OM image of the studied m-plane GaN film. The anisotropic surface morphology exhibits many pyramidal hillocks<sup>13</sup> elongated and aligned along the *x*-direction like the ones observed in thin films grown on low-defect-density m-plane GaN substrates.<sup>13</sup> In addition, a careful inspection of the micrograph in Fig. 1(a) reveals a high density of fine lines (stripelike features) parallel to the *y*-direction, i.e., orthogonal to these elongated pyramidal hillocks.<sup>13</sup>

A detailed topography of the m-plane GaN film is obtained by AFM as shown in Fig. 1(b). The fine lines oriented along the *y*-direction in the OM image [Fig. 1(a)] are now clearly visible. This kind of surface morphology is found in most reports in the literature,<sup>4–8</sup> in which the surface stripes are taken to be oriented along [11 $\bar{2}$ 0]. For a comparison with the surface morphology of our sample, it remains to be clarified whether or not the *y*-direction in Fig. 1 is parallel to [11 $\bar{2}$ 0]. Furthermore, the surface morphology of the LAO substrate does not show any preferred stripe features indicat-

<sup>a)</sup>Author to whom correspondence should be addressed. Electronic mail: krwang@pdi-berlin.de.

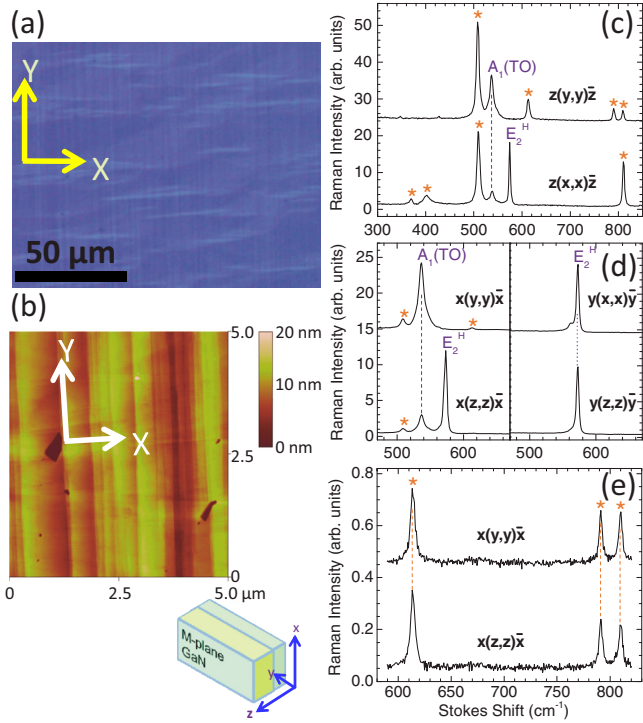


FIG. 1. (Color online) (a) Optical micrograph of the m-plane GaN film grown on LAO. (b) AFM image of the same m-plane GaN film together with the corresponding coordinate system, where the striplike features are parallel to the  $y$ -direction. Raman spectra acquired from (c) the sample surface as well as (d) and (e) different cleaved edges. The scattering geometries are indicated by the notation  $u(v,w)s$ , where  $u(s)$  denotes the direction and  $v(w)$  the linear polarization of the incident (scattered) light. The asterisks refer to Raman peaks originating from the LAO substrate.

ing that the surface observed here is not a replicate of the substrate.

Raman scattering is widely used to investigate hexagonal wurtzite GaN films grown on sapphire substrates.<sup>14</sup> According to the polarization selection rules, the scattering configurations, for which the  $E_2^H$ ,  $A_1(\text{TO})$ , and  $A_1(\text{LO})$  phonon modes can be observed, are listed in Table I. TO and LO refer to the transverse and longitudinal optical phonon modes, respectively. Using a reference frequency of  $568 \text{ cm}^{-1}$  with a value of  $2.7 \text{ cm}^{-1}/\text{GPa}$  as the linear proportionality factor between the shift in the  $E_2^H$  phonon mode and the in-plane biaxial stress,<sup>15</sup> we determine an average compressive stress of 1.85 GPa in our sample.

Figure 1(c) displays Raman spectra acquired in the back-scattering geometry from the sample surface for the configurations  $z(y,y)\bar{z}$  and  $z(x,x)\bar{z}$ , whereas spectra recorded from two cleaved edges are shown in Fig. 1(d) for certain scattering configurations. All spectra clearly exhibit either the  $E_2^H$  or

the  $A_1(\text{TO})$  phonon line (or both) from the GaN film. The  $A_1(\text{LO})$  phonon mode is detected in the configurations  $y(x,x)\bar{y}$  and  $y(z,z)\bar{y}$  but with rather small intensity. Considering the appearance of the phonon lines for different scattering geometries, the selection rules given in Table I are exactly fulfilled only for the following assignments:  $x=a=[1\bar{1}20]$ ,  $y=c=[0001]$ , and  $z=m=[1\bar{1}00]$ . The Raman spectra of the LAO phonon modes (marked by asterisks) for the configurations  $x(y,y)\bar{x}$  and  $x(z,z)\bar{x}$  are nearly identical as shown in Fig. 1(e). This condition is only fulfilled for back-scattering along the  $c$ -axis of LAO with a four-fold symmetry of the  $P4_12_12$  tetragonal crystal.<sup>4,16</sup> Thus, our observation reveals that the  $c$ -axis of the LAO substrate corresponds to the  $x$ -direction in Fig. 1. Therefore, we identify the epitaxial relationship in our sample as  $\text{GaN}(1\bar{1}00)\parallel\text{LAO}(100)$  and  $\text{GaN}[1\bar{1}20]\parallel\text{LAO}[001]$ , as already found in previous reports.<sup>1,4,5,17</sup>

The most important finding of our Raman data is the fact that the stripes observed in the AFM images [cf. Fig. 1(b)] are oriented along the  $c$ -axis of the epitaxial m-plane GaN film [ $y=c$  in Fig. 1(b)]. This orientation relationship is also in agreement with our TEM analysis (not shown here).

Recently, the physical picture of the adatom kinetics that deals with anisotropic crystal growth has been obtained using DFT (Ref. 9) after nearly a decade of heteroepitaxial growth of m-plane GaN on LAO.<sup>1</sup> However, the predicted surface morphology of the m-plane GaN film based on the adatom kinetics does not support our findings. In addition, BPSFs are planar defects, which are often observed in m-plane GaN films and might be the cause of the striplike features parallel to  $[1\bar{1}20]$  as discussed in many reports.<sup>6,8,10</sup> However, stripes along the  $c$ -axis  $[0001]$ , as observed in our case, cannot be explained by the presence of BPSFs.<sup>5,6,8,10</sup>

The cross-sectional high-resolution TEM image of the GaN/LAO interface that is taken along the  $[1\bar{1}20]$  zone axis (Fig. 2) clearly reveals an additional 2-nm-thick single crystalline interlayer at the GaN/LAO interface. Both x-ray reflectivity and TEM investigations indicate that the interlayer consists of AlN, where the two heterointerfaces AlN/LAO and GaN/AlN are formed. Therefore, the reason for the different surface morphology of our m-plane GaN films might be connected to the formation of the interlayer. This result is important because the barriers for the Ga adatom diffusion on  $c$ -plane GaN and AlN are known to be different,<sup>18</sup> which may greatly affect the adatom kinetics during the nucleation and coalescence processes that lead to the formation of an anisotropic surface.

In general, the in-plane strain may also play a role in the solid diffusion processes.<sup>11,19</sup> The theoretical in-plane lattice

TABLE I. Raman geometries, for which the optical phonon modes  $E_2^H$ ,  $A_1(\text{TO})$ , and  $A_1(\text{LO})$  are observable (O) or missing (X) in the corresponding spectra based on the selection rules (Ref. 14). The orientation of the  $c$ -axis and the two orthogonal directions are denoted by  $c=[0001]$ ,  $m=[1\bar{1}00]$ , and  $a=[1\bar{1}20]$ . For the sample studied here, the measured (strain free)  $E_2^H$ ,  $A_1(\text{TO})$ , and  $A_1(\text{LO})$  phonon lines are  $573$  ( $567.6$ )  $\text{cm}^{-1}$ ,  $536$  ( $531.8$ )  $\text{cm}^{-1}$ , and  $740$  ( $734$ )  $\text{cm}^{-1}$ , respectively. The strain-free values are taken from Ref. 14.

Phonon mode	$c(a,a)\bar{c}$ $y(x,x)\bar{y}$	$c(m,m)\bar{c}$ $y(z,z)\bar{y}$	$m(a,a)\bar{m}$ $z(x,x)\bar{z}$	$m(c,c)\bar{m}$ $z(y,y)\bar{z}$	$a(c,c)\bar{a}$ $x(y,y)\bar{x}$	$a(m,m)\bar{a}$ $x(z,z)\bar{x}$
$E_2^H$	O	O	O	X	X	O
$A_1(\text{TO})$	X	X	O	O	O	O
$A_1(\text{LO})$	O	O	X	X	X	X

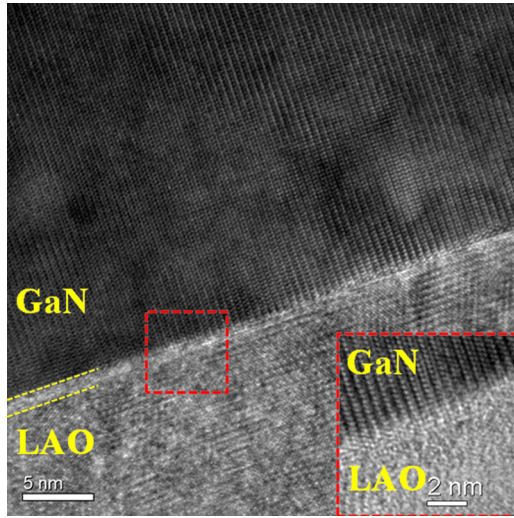


FIG. 2. (Color online) Cross-sectional HRTEM image of the GaN/LAO interface ( $[11\bar{2}0]$  zone axis), where the AlN interlayer is indicated by the dashed lines. A magnified image of the interface marked by the dashed box is shown in the inset.

mismatch values ( $f$ ) of GaN/LAO are  $f_a = -1.6\%$  and  $f_c = -0.3\%$ , while for AlN/LAO and GaN/AlN these values are  $f_a = +0.9\%$  and  $f_c = +3.7\%$  as well as  $f_a = -2.5\%$  and  $f_c = -4.2\%$ , respectively. The lattice mismatch  $f$  is defined as  $(a_{\text{sub}} - a_{\text{epi}})/a_{\text{sub}}$  where  $a_{\text{sub}}$  and  $a_{\text{epi}}$  are the lattice constants of the substrate and the epitaxial layer, respectively. In other words, when the strain ( $\epsilon$ ) is defined as  $\epsilon = (a_{\text{epi}} - a_0)/a_0$  with  $a_0$  denoting the theoretical unstrained lattice constant, the strain components of GaN grown on LAO are expected to be compressive along both the  $c$ - and  $a$ -axis ( $\epsilon_{a\text{-GaN}} < 0$  and  $\epsilon_{c\text{-GaN}} < 0$ ).

In contrast,  $m$ -plane AlN films have been grown on SiC substrates using MBE (Ref. 20) and HVPE (Ref. 21) where the stripes are parallel to  $[11\bar{2}0]$ .<sup>20,21</sup> Using the data provided in these publications,<sup>20,21</sup> we find that the in-plane lattice mismatch values for the MBE-grown AlN on SiC substrates are  $f_a = -0.8\%$  and  $f_c = +0.6\%$ ,<sup>20</sup> while for the ideal case of HVPE-grown films the components are  $f_a = -1.01\%$ , and  $f_c = +1.13\%$ .<sup>21</sup> These data imply that the strain parallel to the  $a$ -axis ( $[11\bar{2}0]$ ) is compressive ( $\epsilon_{a\text{-AlN}} < 0$ ), while the strain along the  $c$ -axis ( $[0001]$ ) is tensile ( $\epsilon_{c\text{-AlN}} > 0$ ). This may lead to the formation of stripes parallel to the  $a$ -axis  $[11\bar{2}0]$  (Refs. 20 and 21) due to the anisotropic component of this mixed strain state, which affects the nucleation coalescence during growth. Nevertheless, the AlN grown on SiC is quite different compared to AlN on LAO, where both  $a$ - and  $c$ -axis exhibit tensile strains (i.e.,  $\epsilon_{a\text{-AlN}} > 0$ ,  $\epsilon_{c\text{-AlN}} > 0$ ). Note that this AlN interlayer is only 2 nm thick. Therefore, it is difficult to observe any changes in the AFM surface scan. However, the difference of the strain state between AlN on SiC and AlN on LAO may result in different surface morphologies, when a thick GaN film is grown on it.

In the case of Ga adatom diffusion on  $m$ -plane GaN, it is unclear whether or not strain-induced changes in the diffusion barriers can overcome the existing difference between the energy barriers (0.72 eV) along the two different crystal orientations.<sup>9</sup> In addition, the barriers for the Ga adatom dif-

fusion on nonpolar AlN are unknown. Therefore, further work is necessary to fully understand the formation mechanism for the specific surface morphology observed in our case.

In conclusion, an unusual orientation of the surface stripes parallel to the  $c$ -axis is observed for  $m$ -plane GaN films grown on LAO by a three-step MOVPE technique. These stripes are neither (i) a replication of the substrate morphology nor (ii) caused by BPSFs. Instead, the stripe formation along  $[0001]$  is attributed to the change in the Ga adatom kinetics due to the presence of a 2-nm-thick AlN interlayer observed at the GaN/LAO interface. Our results demonstrate that the striated surface of  $m$ -plane GaN is highly dependent on the technique and conditions of growth. Therefore, our investigation may give a better understanding of the strain-induced adatom kinetics during the anisotropic growth of  $m$ -plane GaN.

We gratefully acknowledge financial support by the Deutsche Forschungsgemeinschaft (DFG) under Grant No. KA 1738/3-1. The authors would like to thank T. Flisikowski for a critical reading of the manuscript and O. Brandt, U. Jahn, Y. Takagaki, and V. Kaganer for helpful discussions.

- <sup>1</sup>P. Waltereit, O. Brandt, A. Trampert, H. T. Grahn, J. Menniger, M. Ramsteiner, M. Reiche, and K. H. Ploog, *Nature (London)* **406**, 865 (2000).
- <sup>2</sup>S. Chichibu, T. Azuhata, T. Sota, and S. Nakamura, *Appl. Phys. Lett.* **69**, 4188 (1996).
- <sup>3</sup>T. Takeuchi, S. Sota, M. Katsuragawa, M. Komori, H. Takeuchi, H. Amano, and I. Akasaki, *Jpn. J. Appl. Phys., Part 2* **36**, L382 (1997).
- <sup>4</sup>P. Waltereit, O. Brandt, M. Ramsteiner, R. Uecker, P. Reiche, and K. H. Ploog, *J. Cryst. Growth* **218**, 143 (2000).
- <sup>5</sup>Y. J. Sun, O. Brandt, U. Jahn, T. Y. Liu, A. Trampert, S. Cronenberg, S. Dhar, and K. H. Ploog, *J. Appl. Phys.* **92**, 5714 (2002).
- <sup>6</sup>R. R. Vanfleeter, J. A. Simmons, H. P. Maruska, D. W. Hill, M. M. C. Chou, and B. H. Chai, *Appl. Phys. Lett.* **83**, 1139 (2003).
- <sup>7</sup>O. Brandt, Y. J. Sun, L. Däweritz, and K. H. Ploog, *Physica E (Amsterdam)* **23**, 339 (2004).
- <sup>8</sup>B. A. Haskell, A. Chakraborty, F. Wu, H. Sasano, P. T. Fini, S. P. DenBaars, J. S. Speck, and S. Nakamura, *J. Electron. Mater.* **34**, 357 (2005).
- <sup>9</sup>L. Lymperakis and J. Neugebauer, *Phys. Rev. B* **79**, 241308 (2009).
- <sup>10</sup>A. Hirai, B. A. Haskell, M. B. McLaurin, F. Wu, M. C. Schmidt, K. C. Kim, T. J. Baker, S. P. DenBaars, S. Nakamura, and J. S. Speck, *Appl. Phys. Lett.* **90**, 121119 (2007).
- <sup>11</sup>G. S. Kim, J. S. Tse, and D. D. Klug, *Chem. Phys. Lett.* **400**, 74 (2004).
- <sup>12</sup>C. Mauder, L. Rahimzadeh Khoshroo, H. Behmenburg, B. Reuters, M. Bösing, M. V. Rzheutskii, E. V. Lutsenko, G. P. Yablonskii, J. F. Woitok, M. M. C. Chou, M. Heuken, H. Kalisch, and R. H. Jansen, *Phys. Status Solidi C* **6**, S482 (2009).
- <sup>13</sup>A. Hirai, Z. Jia, M. C. Schmidt, R. M. Farrell, S. P. DenBaars, S. Nakamura, J. S. Speck, and K. Fujito, *Appl. Phys. Lett.* **91**, 191906 (2007).
- <sup>14</sup>H. Harima, in *III-Nitride Semiconductors Optical Properties*, edited by M. O. Manasreh and H. X. Jiang (Taylor & Francis, New York, 2002), Vol. I, pp. 283–331.
- <sup>15</sup>V. Y. Davydov, N. S. Averkiev, I. N. Goncharuk, D. K. Nelson, I. P. Nikitina, A. S. Polkovnikov, A. N. Smirnov, M. A. Jacobsen, and O. K. Semchinova, *J. Appl. Phys.* **82**, 5097 (1997).
- <sup>16</sup>J. F. Nye, *Physical Properties of Crystals: Their Representation by Tensors and Matrices* (Oxford University Press, Oxford, 1985), pp. 82–149.
- <sup>17</sup>B. Rau, P. Waltereit, O. Brandt, M. Ramsteiner, K. H. Ploog, J. Puls, and F. Henneberger, *Appl. Phys. Lett.* **77**, 3343 (2000).
- <sup>18</sup>V. Jindal and F. Shahedipour-Sandvik, *J. Appl. Phys.* **105**, 084902 (2009).
- <sup>19</sup>E. Penev, P. Kratzer, and M. Scheffler, *Phys. Rev. B* **64**, 085401 (2001).
- <sup>20</sup>R. Armitage, J. Suda, and T. Kimoto, *Appl. Phys. Lett.* **88**, 011908 (2006).
- <sup>21</sup>J. J. Wu, K. Okumura, K. Okumura, H. Miyake, K. Hiramatsu, Z. T. Chen, and T. Egawa, *J. Cryst. Growth* **312**, 490 (2010).